Key Engineering Materials Vols. 270-273 (2004) pp. 35-40
online at http://www.scientific.net

Residual Stress Assessment in API X65 Pipeline Welds by Non-destructive Instrumented Indentation

Yun-Hee Lee[1], Dongil Kwon[1], Jae-il Jang[2] and Woo-sik Kim[3]

[1] School of Materials Science & Engineering, Seoul National University, Seoul 151-742 Korea

[2] Frontics, Inc., 10th Floor, Baikgwang Bldg., Bongchun-10-dong, Seoul 151-060, Korea

[3] Research & Development Center, Korea Gas Corporation, Ansan 425-150, Korea

Keywords: Welding Residual Stress, Instrumented Indentation, API X65 Pipeline Steel, Non-destructive Testing

Abstract. Conventional residual stress-measurement methods are difficult to use in industrial structures largely because of their complexity and destructive nature. In particular, the rapid microstructural gradients across welds impede a quantitative assessment of residual stress. An instrumented indentation technique has been developed to overcome the current problems in measuring the residual stress. Here this instrumented indentation technique was used to characterize the residual stress in API X65 steel welds in a natural gas transmission pipeline. The difference in indentation load between the stressed and unstressed regions at a fixed penetration depth was converted to a quantitative residual stress value through an analytical procedure. The stress distribution assessed across the welds agreed roughly with that from destructive saw-cutting tests. The discrepancy in absolute stress values from the two methods was considered to arise from the effects of microstructural difference and stress directionality in the welds.

Introduction

The quantitative measurement of welding residual stress is very important for the safe operation and economical maintenance of industrial structures and facilities such as gas/oil transmission pipelines, power plants, petrochemical plants, and so on. Over the last few decades, various lab-scale stress-measurement methods have been developed [1]. Destructive hole-drilling and saw-cutting methods are sensitive to macroscopic stress and evaluate the residual stress quantitatively without any reference sample, but they have limitations in industrial applications due to their destructive characteristics and the possibility of creating a new stress state by material removal. Thus, such nondestructive methods as X-ray and neutron diffraction, ultrasonic method, and Barkhausen noise have been investigated to establish relationships between the physical or crystallographic stress-detection parameter and the residual stress. However, these techniques are difficult to apply to welds with rapid microstructural gradients because the stress-detection parameter is also highly sensitive to metallurgical factors.

Initial indentation studies for measuring residual stress focused on deriving the stress dependency of the contact hardness [2]. However, the stress-induced alteration in the hardness was less than 10% of its value in the unstressed specimen [3], so that the use of the contact hardness as a residual stress parameter was dubious. Recently, an instrumented indentation technique that measures elastic/plastic deformation behavior beneath a rigid indenter as a curve of indentation load versus indenter penetration depth has been developed and applied to evaluate various mechanical properties such as contact hardness, elastic modulus [4], yield and tensile strengths, work-hardening index [5] and fracture toughness [6]. The stress sensitivity and application potential of this technique had been recognized earlier; however, the relevant studies were tentative and somewhat empirical for a good while. Tsui et al. [3], studying the influence of in-plane stress on indentation plasticity by investigating both the shape of the indentation curve and the contact impressions, reported that hardness is invariant regardless of the applied stress within the elastic limit. An indentation model

proposed by Suresh and Giannakopoulos [7] yielded a theoretical relationship between the residual stress and the ratio of contact areas from stressed and unstressed samples. However, their analysis does not extract the influence of the residual stress on plastic deformation clearly, and direct measurement of the contact area for each stress state is a troublesome procedure.

Another approach proposed by Lee and Kwon [8] was based on the stress-insensitive hardness and a concept of shear plasticity. In this study, the instrumented indentation technique was combined with Lee and Kwon's model [8] and applied to the nondestructive and quantitative characterization of welding residual stresses in natural gas transmission pipelines. The stress values estimated were compared with results from the destructive saw-cutting technique.

Stress Analysis from a Load Shift in the Indentation Curve

The residual stress near welds is assumed to be in an equi-biaxial state ($\sigma_{res,x} = \sigma_{res,y} = \sigma_{res}$, $\sigma_{res,z} = 0$) and uniform within the near-surface region (about three times greater than the indentation depth). A load shift at the fixed depth h_t in Fig. 1 is sensitive to the sign and absolute magnitude of the residual stress: a positive or negative shift represents compressive or tensile stress, respectively. This load shift was analyzed in terms of the residual-stress-induced normal load L_{res} based on the concept of shear plasticity [8].

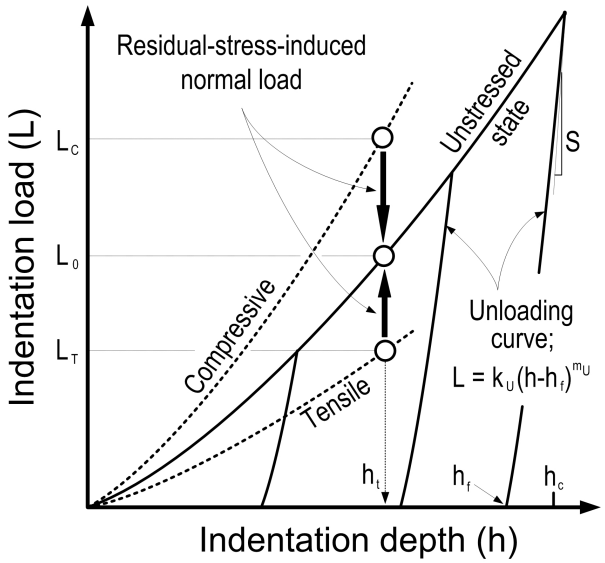

Fig. 1. Theoretical analysis of the instrumented indentation curve and its shape variation as influenced by stress state.

A surface-normal deviator stress component ($\sigma_{33}^{D} = -2\sigma_{res}/3$) is obtained from the equi-biaxial residual stress by subtracting a hydrostatic stress and is added directly to the indentation pressure. L_{res} is defined as a product of the selected deviator stress component and contact area A_C [8].

The contact area is generally calculated from the unloading or elastic recovery curve by using the Oliver and Pharr's contact analysis [4] in Eq. (1) and the indenter geometry (rather than optical measurement):

$$h_C = h_{max} - 0.72\frac{L_{max}}{S}, \tag{1}$$

where h_C is the contact depth and S is the experimentally measured contact stiffness (i.e., it corresponds to the gradient of the tangent to the unloading curve at the maximum indentation depth

h_{max}). The contact area A_C is expressed as $24.5h_C^2$ for a Vickers pyramidal indenter. The contact depth or area of a stressed sample also can be analyzed from the unloading curve. However, a recent study on the indentation marks formed at various stress states has found that the contact area is independent of the pre-existing elastic stress state [3], although the shape of the indentation unloading curve is sensitive to the stress state. This means that the unloading curve produced in a stressed state cannot give accurate contact information due to additional stress-induced deformation effects and that a unique contact area exists corresponding to a particular indentation load regardless of the stress state. Thus the contact depth analysis was carried out for the unstressed sample only and the contact information derived was used in all subsequent analyses without considering the pre-existing stress state of the sample.

The response of the contact area corresponding to the relaxation in the indentation load from the stressed to the unstressed states in Fig. 1 was also investigated by assuming a reversible recovery during a depth-controlled stress relaxation [8]. The indentation load and contact area for the tensile stressed state must be L_T and A_C^T, smaller than L_0 and A_C^0 for the unstressed state, to satisfy the stress-independent contact hardness at the fixed indentation depth h_t. A gradual relaxation of the tensile stress causes a rebounding force that pushes the indenter out from the surface [8]. However, the rebounding force appears as the increases in the indentation load ($L_T \rightarrow L_0$) and contact area ($A_C^T \rightarrow A_C^0$) because the indentation depth is constant. The sign of the residual-stress-induced normal load L_{res} was reversed during the stress relaxation, and this continuous stress relaxation was expressed as an integral equation in Eq. (2).

$$L_0 = L_T + L_{res} = L_T + \frac{2}{3}\int_{L_T}^{L_0} d(\sigma \cdot A_C) \ . \qquad (2)$$

The relaxation behavior of the residual stress from the initial value of σ_{res} to the final stress-free state is assumed to be linear, and the response of A_C during the stress relaxation is simply expressed as the indentation load L divided by the contact hardness H. Finally, an equation for the residual stress is derived in terms of the indentation load and contact area as:

$$\sigma_{res} = -\frac{3}{2}\frac{L_{res}}{A_C^T} \ . \qquad (3)$$

Experimental Details

Girth weld samples of natural gas transmission pipeline were used for the instrumented indentation and saw-cutting tests. Two 15.0-mm-thick API X65 steel pipes, with base material of chemical composition 0.08C-0.019P-1.45Mn-0.003S-0.31Si, were machined into V-groove configuration and were welded first by gas tungsten arc welding (GTAW) with AWS ER70S-G electrode and then by shielded metal arc welding (SMAW) with AWS E9016-G electrode. The pipes were preheated to 100ºC before welding, while post-weld heat treatment (PWHT) was not performed for the welds. No significant defects were detected in the completed welds by nondestructive X-ray examination. The welding bead was removed flat and the weld surface was then mechanically ground using emery paper #1000 in order to eliminate effects of surface tilting or roughness in the instrumented indentation results.

A commercial AIS 3000R manufactured by Frontics, Inc., Seoul, Korea with depth and load resolutions of 0.1 μm and 14.7 mN was used for the instrumented indentation tests. The tests were carried out on two regions, near welds and remote base metal (more than 80 mm from the fusion line),

respectively, for the residually stressed and unstressed states, as shown in Fig. 2. The maximum applied load and testing speed were 294 N and 0.2 mm/min. Indentation arrays of more than 15 points were made across the welds at 5 mm intervals from the weld line center. A multiple indenting procedure with three load-unload cycles at maximum loads of 98, 196, and 294 N was applied to the unstressed base metal to obtain the residual-stress-induced load shift and contact properties at different depth or load steps. The microstructural variation near welds was also observed after the tests.

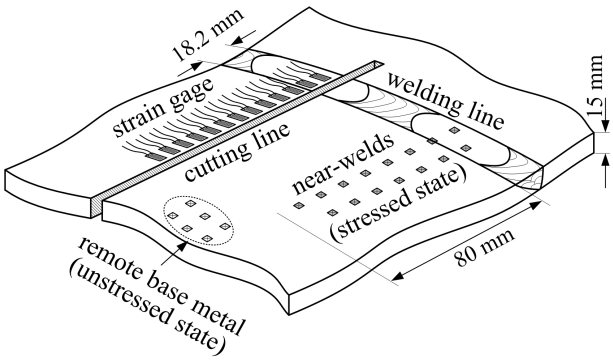

Fig. 2. The instrumented indentation and saw-cutting tests on the girth welds sample.

Residual stress was calculated by inserting the contact information for indentation curves from the near-weld stressed region and unstressed base metal into Eq. (3). To measure the residual stress parallel to the welding line by the saw-cutting method and to compare the obtained results with the stress distributions of the indentation technique, we attached strain gauges across the welding line and cut ahead of them, as shown in Fig. 2. The relaxation strains were converted to the residual stresses by multiplying the Young's modulus of API X65 steel, 210 GPa.

Results and Discussion

Metallurgical boundaries among weld metal, heat-affected zone (HAZ), and base metal were identified by optical observation. The width of the weld metal was about 18.2 mm and the boundary between the HAZ and base metal was approximately 4.8 mm from the fusion line (we assumed that the total HAZ width is twice that of the HAZ region accompanying the microstructural change). The instrumented indentation curves obtained from the near-weld region are superposed on that of the unstressed base metal in Fig. 3. Indentation loading curves are fitted in a power-law function, and the stress-induced load shifts at the given depth 50 μm are calculated in Table 1.

Table 1. Power-law fitting equation of indentation loading curve from each testing region.

Distance of testing region from fusion line [mm]	Loading curve fitted in power-law function	Load shift at indentation depth of 50 μm [N]
Weld metal (-3.2)	$L = 0.087\ h^{1.935}$	-12.4
Heat-affected zone (+4.8)	$L = 0.116\ h^{1.896}$	+12.0
Base metal (+9.3)	$L = 0.134\ h^{1.859}$	+11.9
Unstressed base metal (+85.6)	$L = 0.114\ h^{1.884}$	-

The indentation load is lower in the weld metal (-3.2 mm from the fusion line) than in the unstressed base metal at a given depth, and increases in the base metal near the welds (+9.3 mm from the fusion line). Since the indentation pressure is compressive and acts perpendicularly to the surface, the tensile applied stress increases the magnitude of the shear stress beneath the indenter relative to

Title of Publication (to be inserted by the publisher)

the unstressed specimen. The increase of the shear stress under tensile stress enhances indentation plasticity, thereby producing a lower indentation load than in the unstressed state for the same indentation depth. If mechanical and metallurgical differences of the weld metal from the base metal are neglected, the total load shift in the weld metal reflects only the effects of the residual stress; the weld metal is in a tensilely stressed state, while the base metal near the welds is in a state of compressive residual stress. The indentation curve of the base metal, obtained from the region +74.9 mm from the fusion line, almost matches that of the unstressed API X65 base metal, showing that the influence of welding residual stress on indentation plasticity fades away with increasing distance from the fusion line.

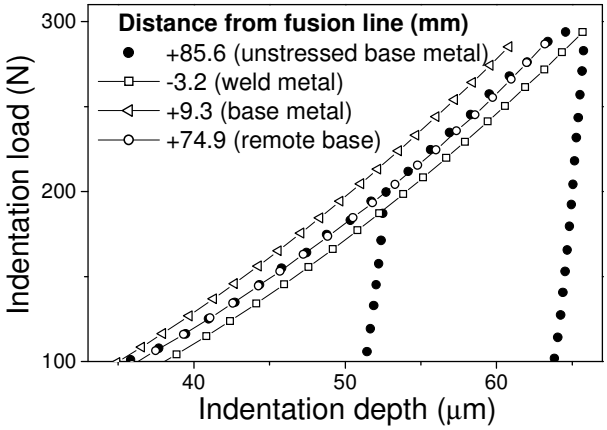

Fig. 3. Superposition of instrumented indentation curves from near-weld region on that of the unstressed base metal.

The measured indentation depth at 294 N for the unstressed base metal was reproducible within a standard deviation of ±0.3 μm. The contact depth, analyzed from each unloading step using the Oliver and Pharr's method [3], was converted to the contact area as shown in Table 2.

Table 2. Contact properties evaluated from unloading curve analysis for unstressed base metal.

Applied load [N]	Indentation depth [μm]	Contact depth [μm]	Contact area [μm^2]
294	65.1 ± 0.3	63.4 ± 0.2	98593.1 ± 633.2
196	51.7 ± 0.2	50.1 ± 0.3	61482.5 ± 677.3
98	34.8 ± 0.2	33.6 ± 0.2	27723.9 ± 334.9

The residual stress distribution near the welds was assessed by inserting the calculated data into Eq. (3); it is compared in Fig. 4 with results obtained by the saw-cutting technique. From a rough comparison, the residual stresses obtained by the two methods vary similarly across the welds. The tensile residual stress in the weld metal decreased abruptly across the HAZ and changed into compressive residual stress in the base metal near the welds, and then gradually converged to the stress-free state at the remote base metal region. A detailed comparison shows that the residual stress in the weld metal was greatly overestimated compared with the results of the saw-cutting method. This phenomenon can be explained metallurgically: the shifts in the indentation curves for the weld metal and HAZ from that of the unstressed base metal imply the combined influences of the residual stress, microstructural variations, mechanical strength difference, and so on.

To evaluate the influence of the residual stress only in these regions, stress-relief annealing at 600ºC and 2hr was performed on the weld specimen. The effectiveness of this thermal annealing, usually known as PWHT, has been described in a previous study [9]. The residual stress distribution

within the weld metal and HAZ was recalculated by obtaining the stress-free indentation curve corresponding to each microstructural region, and is superposed on the already analyzed results in Fig. 4. As expected, the recalculated stress values for the weld metal and HAZ were more similar to those for the saw-cutting technique.

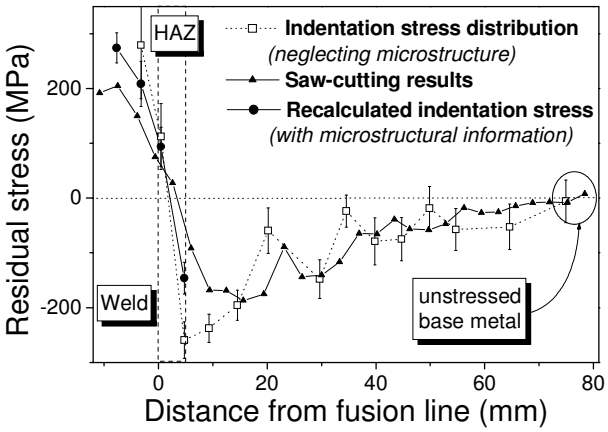

Fig. 4. Comparison of the stress distributions from the saw-cutting and the proposed indentation tests; neglecting microstructural differences can cause notable differences in absolute stress values in the weld metal and HAZ.

However, the discrepancy of the stress directionality can also influence the results; an equi-biaxial in-plane state was assumed here for the welds, while the real stress distributions near the welds include both longitudinal ($\sigma_{res,x}$) and transverse stress ($\sigma_{res,y}$) with different magnitudes and stress signs. Thus, further research on the principal stress near the welds must be done with a view to improving the indentation technique.

Conclusions

The instrumented indentation technique was applied to the evaluation of welding residual stress in API X65 steel welds in natural gas transmission pipeline. Comparison with the saw-cutting results showed that the instrumented indentation test has potential in the nondestructive assessment of welding residual stresses in industrial structures. However, it is indispensable for the accurate and quantitative stress evaluation to obtain both the stress-free indentation curve corresponding to each microstructural region and the principal stress information for the tested sample.

References

[1] J. Lu, M.R. James and G. Roy: *Handbook of Measurement of Residual Stresses* (Fairmont Press, Inc., Lilburn, GA, USA 1996).

[2] G. Sines and R. Calson: ASTM Bulletin, February (1952), p. 35.

[3] T.Y. Tsui, W.C. Oliver and G.M. Pharr: J. Mater. Res. Vol. 11 (1996), p. 752.

[4] W.C. Oliver and G.M. Pharr: J. Mater. Res. Vol. 7 (1992), p. 1564.

[5] J.-H. Ahn and D. Kwon: J. Mater. Res. Vol. 16 (2001), p. 3170.

[6] Y.-H. Lee and D. Kwon: Key Eng. Mater. Vol. 161-163 (1999), p. 569.

[7] S. Suresh and A.E. Giannakopoulos: Acta Mater. Vol. 46 (1998), p. 5755.

[8] Y.-H. Lee and D. Kwon: Scripta Mater. Vol. 49 (2003), p. 459.

[9] A.G. Olabi and M.S.J. Hashmi: J. Mater. Process. Technol. Vol. 56 (1996), p. 552.